

The Primary Photodynamics of Aqueous Nitrate: Formation of Peroxynitrite

Dorte Madsen,[†] Jane Larsen,[‡] Svend Knak Jensen, Søren R. Keiding, and Jan Thøgersen*

Contribution from the Department of Chemistry, University of Aarhus, Langelandsgade 140, DK-8000, Aarhus, Denmark

Received February 24, 2003; Revised Manuscript Received October 13, 2003; E-mail: thogersen@chem.au.dk

Abstract: We have examined the photochemical reactions occurring after irradiation at 200 nm of the aqueous nitrate ion, NO_3^- (aq). Using femtosecond transient absorption spectroscopy over the range 194–388 nm, we have characterized the formation and subsequent relaxation of the primary photoproducts of nitrate photolysis. The dominant photoproduct is the *cis*-isomer of peroxynitrite, which accounts for 48% of the excited state molecules initially produced. A slightly smaller fraction, 44%, of the excited molecules return to the electronic ground state of NO_3^- and relax to the vibrational ground state in 2 ps. The remaining 8% of the molecules initially excited react via the $\bullet\text{NO} + \bullet\text{O}_2^-$ or the $\text{NO}^- + \text{O}_2$ dissociation channels. Formation of NO_2^- and $\bullet\text{NO}_2$ is not observed, suggesting that the previous observations of these species in steady-state photolysis are caused by reactions occurring on a longer time scale.

Introduction

The photochemistry of the nitrate ion, NO_3^- , has been studied extensively since the early experiments by Thiele back in 1907.¹ Later work in this area has included modeling of the Martian surface to explain the result of the Viking Lander experiments,² while more recent photochemical investigations of nitrate have been spurred by its involvement in the disinfection of drinking water.^{3,4} Currently, there is an intense interest in the biochemistry of the nitrate isomer peroxynitrite, ONOO^- , since it has been implicated in the onset of numerous diseases.⁵ Physiologically, ONOO^- is formed by reaction of superoxide, $\bullet\text{O}_2^-$, with nitric oxide, $\bullet\text{NO}$. The need for additional information about these detrimental processes warrants detailed investigations of reactions involving these species. The present study is thus motivated by the possible formation of ONOO^- , $\bullet\text{O}_2^-$, and $\bullet\text{NO}$ from far-ultraviolet photolysis of the nitrate ion.^{6–9}

Considering that the chemistry of the nitrate ion has been studied for a long time, it may seem surprising that uncertainty concerning its primary photochemistry still prevails. According

to a recent comprehensive review by Mack and Bolton,³ the overall products resulting from the photolysis of aqueous NO_3^- are NO_2^- and O_2 . Nevertheless, fundamental issues regarding the kinetics of primary and intermediate reactions remain unsolved. This is, in part, due to the complexity of the nitrate chemistry, but also is a consequence of secondary reactions obscuring the initial steps of the nitrate photolysis in studies with modest time resolution. In the present investigation, the photodynamics of aqueous nitrate are studied by far-UV transient absorption spectroscopy with femtosecond time resolution, thus facilitating the characterization of the primary photoproducts.

The isolated nitrate ion is planar (D_{3h}) with the excess negative charge delocalized over the molecule. The lowest excited states of nitrate are ${}^3A_1'$, ${}^1A_1''$, ${}^3E'$, and ${}^1E'$ with Franck–Condon excitation maxima of 3.6, 4.1, 4.7, and 6.0 eV, relative to the X^1A_1' ground state.¹⁰ In polar solvents, the distribution of solvent molecules surrounding the nitrate ion tends to localize the negative charge, thereby reducing the symmetry of the ground state to an essentially planar structure with one N–O bond different from the others (C_{2v}) or with all N–O bonds different (C_s).^{11–13} The hydrated nitrate ion has a weak $n \rightarrow \pi^*$ absorption band around 302 nm,¹⁴ and a much stronger $\pi \rightarrow \pi^*$ band with absorption maximum at 200 nm (corresponding to the $X^1A_1' \rightarrow {}^1E'$ transition in D_{3h} symmetry).^{11,15} Excitation of both transitions is accompanied by substantial weakening of

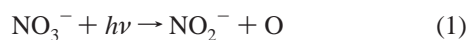
[†] Present address: FOM-Institute for Atomic and Molecular Physics (AMOLF), Kruislaan 407, 1098 SJ Amsterdam, The Netherlands.

[‡] Present address: Department of Chemical Physics, Chemical Centre, Lund University, P.O. Box 124, SE-22100 Lund, Sweden.

- (1) Thiele, H. *Ber. Dtsch. Chem. Ges.* **1907**, *40*, 4914–16.
- (2) Plumb, R. C.; Tantayanon, R.; Libby, M.; Xu, W. W. *Nature* **1989**, *338*, 633–635.
- (3) Mack, J.; Bolton, J. R. *J. Photochem. Photobiol.* **1999**, *A128*, 1–13.
- (4) Mark, G.; Korth, H.-G.; Schuchmann, H.-P.; Sonntag, v. C. *Photochem. Photobiol. A* **1996**, *101*, 89–103.
- (5) Flint, B. M. *Free Radical Biol. Med.* **2002**, *32*, 797–803.
- (6) Papée, H. M.; Petriconi, G. L. *Nature* **1964**, *204*, 142–145.
- (7) Shuali, U.; Ottolenghie, M.; Rabani, J.; Yelin, Z. *J. Phys. Chem.* **1969**, *73*, 3445–3450.
- (8) Barat F.; Gilles, L.; Hickel, B.; Sutton, J. *J. Chem. Soc. A* **1970**, 1982–1986.
- (9) Richard, J.; Bradley, E.; Lanzendorf, McCarthy, M. I.; Orlando, T. M.; Hess, W. P. *J. Phys. Chem.* **1995**, *99*, 11715–11721.

- (10) Nevostuev, V. A. *High Energy Chem.* **1986**, *20*, 329–333.
- (11) Waterland, M. R.; Kelley, A. M. *J. Chem. Phys.* **2000**, *113*, 6760–6773.
- (12) Waterland, M. R.; Stockwell, D.; Kelley, A. M. *J. Chem. Phys.* **2001**, *114*, 6249–6258.
- (13) Shen, M.; Xie, Y.; Schaefer, H. F., III; Deakyne, C. A. *J. Chem. Phys.* **1990**, *93*, 3379–3388.
- (14) Blandamer, M. J.; Fox M. F. *Chem. Rev.* **1970**, *70*, 59–93.
- (15) Maria, H. J.; McDonald, J. R.; McGlynn, S. P. *J. Am. Chem. Soc.* **1973**, *95*, 1050–1056.

the N–O bonds, and breaking of N–O bonds is expected to ensue.^{10,11} However, the dissociation processes following the photoexcitation of aqueous nitrate have had a history of considerable controversy over the past 35 years. Early photolysis studies by Daniels et al.¹⁶ suggested that excitation in the $n \rightarrow \pi^*$ band at 300 nm results in the two primary product channels:



The primary formation of $\bullet\text{NO}_2$ was also reported by Barat et al.⁸ and Shuali et al.⁷ upon excitation of the $\pi \rightarrow \pi^*$ band, whereas the same studies suggested that NO_2^- arises from secondary reactions and not from the direct photodissociation process (eq 1). These findings were later contested by Bayliss and Bucat,¹⁷ who, on the basis of the excitation studies of both the $n \rightarrow \pi^*$ and the $\pi \rightarrow \pi^*$ transition, concluded that NO_2^- (eq 1) rather than $\bullet\text{NO}_2$ (eq 2) is the primary photodissociation process. Still, more recent steady-state photolysis experiments performed at 254 nm (right at the intersection of the $\pi \rightarrow \pi^*$ and $n \rightarrow \pi^*$ absorption bands) indicate that $\bullet\text{NO}_2 + \bullet\text{O}^-$ is the dominant dissociation channel with a quantum yield of 9%, while NO_2^- is produced in much smaller yields of less than 0.1%.⁴ Hence, it appears the photodissociation channels of aqueous nitrate are not well-established.

In addition to photodissociation, numerous photochemical investigations have shown that, upon excitation of the $\pi \rightarrow \pi^*$ band, the nitrate ion can isomerize to peroxyxynitrite:^{6–8}



This photoisomerization could occur directly or by recombination of primary photoproducts. Considering the latter possibility, formation of peroxyxynitrite could in principle occur through reaction of $\bullet\text{NO}_2$ and $\bullet\text{O}^-$. However, experiments using high concentrations of $\bullet\text{O}^-$ scavengers have deemed this reaction channel insignificant.⁴ Likewise, ONOO^- may be formed through reaction of $\text{NO}^- + \text{O}_2$ ^{18–20} or by the radical reaction $\bullet\text{NO} + \bullet\text{O}_2^- \rightarrow \text{ONOO}^-$.^{21–25} So far, however, neither of the reactants involved in these processes have been identified as primary products of the aqueous nitrate photolysis. On the other hand, steady-state photolysis studies of aqueous nitrate,⁴ ammonium nitrate,²⁶ and potassium nitrate²⁷ films suggest that peroxyxynitrite is formed by direct photoisomerization. These findings are supported by resonant Raman spectroscopy of the $\pi \rightarrow \pi^*$ excitation, which indicates that excited-state aqueous nitrate is pyramidal, thus bringing the oxygen atoms closer together and facilitating the ONOO^- formation.^{11,17}

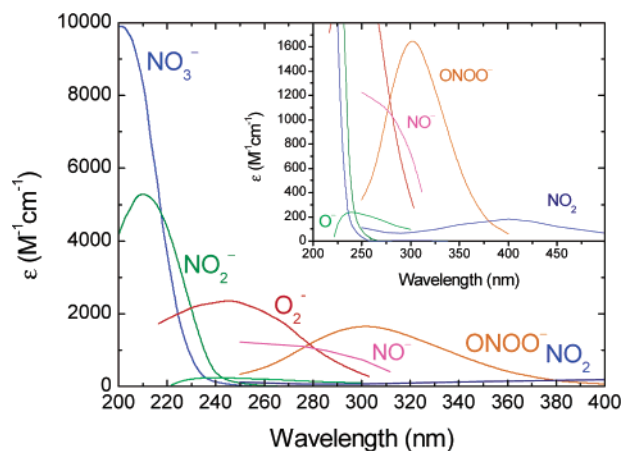


Figure 1. Absorption spectra of the species potentially involved in the primary photolysis of aqueous nitrate.

The femtosecond transient absorption measurements presented in this work produce direct evidence for peroxyxynitrite formation by photoisomerization of nitrate within the solvent cage. The measurements also reveal that the formation of peroxyxynitrite is accompanied by a minor yield of $\bullet\text{O}_2^-$ or NO^- . In contrast, neither NO_2^- nor $\bullet\text{NO}_2$ is identified among the primary photolysis products. Apart from unveiling the primary photochemicals of nitrate, the transient absorption measurements offer a rare opportunity to follow the constitutional isomerization and vibrational relaxation of small molecular ions.

The present investigation of the nitrate photolysis is based on femtosecond transient absorption spectroscopy, which identifies the species involved in the photodynamics by their steady-state absorption spectra, depicted in Figure 1. The spectrum of $\text{NO}_3^-(\text{aq})$ peaks at 200 nm with an extinction coefficient of $\epsilon = 9900 \text{ M}^{-1} \text{ cm}^{-1}$, while $\text{NO}_2^-(\text{aq})$ has a maximum extinction coefficient of $\epsilon = 5500 \text{ M}^{-1} \text{ cm}^{-1}$ at 210 nm.^{3,28} $\bullet\text{NO}_2(\text{aq})$ and $\bullet\text{O}^-(\text{aq})$ both have weak absorption bands ($\epsilon < 250 \text{ M}^{-1} \text{ cm}^{-1}$) with maxima at 400 and 240 nm, respectively,^{29–31} whereas the oxygen atom produced in reaction 1 does not absorb within the spectral range probed. $\bullet\text{NO}(\text{aq})$ absorbs only weakly in the UV–vis region, while its anion, $\text{NO}^-(\text{aq})$, absorbs below 300 nm and has an extinction coefficient of $1200 \text{ M}^{-1} \text{ cm}^{-1}$ at 260 nm.³² Finally, peroxyxynitrite potentially exists as planar *cis*- and *trans*-isomers. The absorption band of *cis*-peroxyxynitrite is centered at 302 nm with a maximum extinction coefficient of $1670 \text{ M}^{-1} \text{ cm}^{-1}$.^{24,33,34} *trans*- ONOO^- has not been observed in aqueous solution, but guided by measurements and calculations on KOONO in solid Ar-matrices, we estimate that the absorption spectrum of *trans*- $\text{ONOO}^-(\text{aq})$ is shifted toward longer wavelengths by ~ 50 nm relative to that of the *cis*-isomer.^{35,36} The extinction coefficient of *trans*- ONOO^- has not been determined.

(16) Daniels, M.; Meyers, R. V.; Belardo, E. V. *J. Phys. Chem.* **1968**, *72*, 389–399.

(17) Bayliss, N. S.; Bucat, R. B. *Aust. J. Chem.* **1975**, *28*, 1865–1878.

(18) Donald, C. E.; Hughes, M. N.; Thompson, J. M.; Bonner, F. T. *Inorg. Chem.* **1986**, *25*, 2676–2677.

(19) Hughes, M. N.; Nicklin, H. G. *J. Chem. Soc. A* **1971**, 164–171.

(20) Hughes, M. N.; *Biochem. Biophys. Acta* **1999**, *1411*, 263–272.

(21) Beckman, J. S.; Beckman, T. W.; Chen, J.; Marshall, P. A.; Freeman, B. A. *Proc. Natl. Acad. Sci. U.S.A.* **1990**, *87*, 1620–1624.

(22) Goldstein, S.; Czapski, G. *Free Radical Biol. Med.* **1995**, *19*, 505–510.

(23) Huie, R. E.; Padmaja, S. *Free Radical Res. Commun.* **1993**, *18*, 195–199.

(24) Kissner, R.; Nauser, T.; Bugnon, P.; Lye, P. G.; Koppenol, W. H. *Chem. Res. Toxicol.* **1997**, *10*, 1285–1292.

(25) Blough, N. V.; Zafiriou, O. C. *Inorg. Chem.* **1985**, *24*, 3504–3505.

(26) Koch, T. G.; Holmes, N. S.; Roddis, T. B.; Sodeau, J. R. *J. Phys. Chem.* **1996**, *100*, 11402–11407.

(27) Plumb, R. C.; Edwards, J. O. *J. Phys. Chem.* **1992**, *96*, 3245–3247.

(28) Fischer, M.; Warneck, P. *J. Phys. Chem.* **1996**, *100*, 18749–18756.

(29) Lymar, S. V.; Schwartz, H. A.; Czapski, G. *J. Phys. Chem. A* **2002**, *106*, 7245–7250.

(30) Grätzel, M. V.; Henglein, A.; Lilie, J.; Beck, G. *Ber. Bunsen-Ges. Phys. Chem.* **1969**, *73*, 646–653.

(31) Rabani, J. *Adv. Chem. Ser.* **1968**, *81*, 131–152.

(32) Seddon, W. A.; Fletcher, J. W.; Sopchysyn, F. C. *Can. J. Chem.* **1973**, *51*, 1123–1130.

(33) Løgager, T.; Sehested, K. *J. Phys. Chem.* **1993**, *97*, 6664–6669.

(34) Hughes, M. N.; Nicklin, H. G. *J. Chem. Soc. A* **1968**, 450–452.

(35) Lo, W.-J.; Lee, Y.-P.; Tsai, J.-H. M.; Beckman, J. S. *Chem. Phys. Lett.* **1995**, *242*, 147–152.

(36) Krauss, M. *Chem. Phys. Lett.* **1994**, *222*, 513–516.

Experimental Section

The double-beam transient absorption spectrometer utilized in this work is improved relative to that of previous studies.³⁷ Briefly, a 1 kHz Titanium-Sapphire laser system emitting 90 fs pulses with a pulse energy of 0.75 mJ is frequency quadrupled to generate the 200 nm pulse used to initiate the photolysis. The $\sim 5 \mu\text{J}$ pump pulse is modulated at 0.5 kHz by a mechanical chopper synchronized to the 1 kHz pulse repetition rate and sent through a scanning delay line and a $\lambda/2$ waveplate before it is focused through the sample by a $f = 50$ cm parabolic mirror. The probe pulses covering the spectral range from 460 to 3000 nm are generated by a two-stage optical parametric amplifier (OPA) pumped at 400 nm. Probe pulses ranging from 230 to 460 nm are produced by frequency doubling the pulses from the OPA in a 0.2 mm BBO crystal, while the spectral region between 214 and 300 nm is covered by frequency mixing the 400 nm pulses with pulses from the OPA. Likewise, mixing the residual 266 nm pulses with OPA pulses generates probe pulses in the spectral range from 194 to 220 nm. The probe beam is then split into a signal and a reference beam. The signal beam is focused onto the sample by an $f = 20$ cm CaF_2 lens and probes the sample inside the area defined by the pump beam. Signal and reference pulses are then detected by matched photodiodes and boxcar integrators before being processed by a digital lock-in amplifier referenced to the 0.5 kHz modulation of the pump pulse.

The sample consisted of a ~ 0.1 mm jet of 0.014 M aqueous KNO_3 solution. The flow was adjusted to give a fresh sample for every laser pulse. No measurable degradation of the KNO_3 solution was observed during the measurements, but to avoid potential build-up of permanent photoproducts the solution was replaced regularly. The reproducibility of the transient absorption data was tested among consecutive scans as well as by repeating the measurements on different days using different samples. From numerous measurements, we found that the data could be measured on a common absorption scale with an uncertainty of less than $\pm 10\%$. The uncertainties quoted in the remainder of this work refer only to uncertainties pertaining to our measurements, as most referenced spectral data are reported without error estimates.

Results

The photoinduced transient absorption, $\Delta A(\lambda, t)$, of aqueous NO_3^- produced by the 200 nm photolysis pulse and measured at 0.2 eV (1613 cm^{-1}) intervals in the spectral range from 194 to 368 nm is presented in the color contour plot of Figure 2. The transient absorption is also depicted at four selected probe wavelengths, 326, 270, 230, and 206 nm, in Figure 3 to clearly display all absorption dynamics. Common to all curves in Figures 2 and 3 is an initial sharp peak, which mainly originates from the coherent absorption of one pump and one probe photon in water.³⁸ On the basis of the prompt response of the two-photon absorption signal, we utilize the position and width of this peak to determine the point of zero delay and the temporal resolution (250 fs), respectively. Additional measurements on aqueous NO_3^- at a probe wavelength of 700 nm (not shown) found no sign of hydrated electrons, indicating that electron photodetachment of $\text{NO}_3^-(\text{aq})$ is insignificant.^{39,40} Finally, measurements performed on neat water showed that photoproducts pertaining to the photolysis of water contribute less than 1 mOD across the investigated spectrum.⁴¹

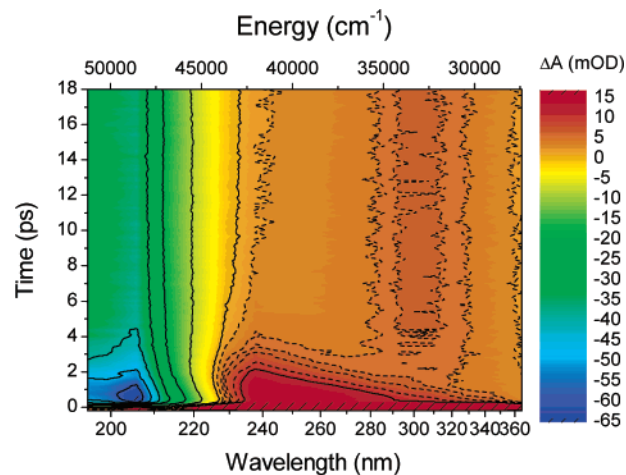


Figure 2. Contour plots of the induced transient absorption of aqueous NO_3^- when excited at 200 nm. The absorption transients cover the initial 18 ps and are measured at 0.2 eV intervals in the spectral range from 194 to 368 nm with 250 fs time resolution. Blue, green, and yellow colors denote negative absorption induced for instance by the disappearance of absorbing species, while orange and red areas indicate increased absorption pertaining to the formation of new species. Thus, the negative absorption with maximum at 206 nm pertains to the removal of ground-state nitrate ions by the photolysis pulse. The red area spanning the first 2 ps in the spectral range from 230 to 360 nm indicates the formation of vibrationally excited NO_3^- molecules, while the induced absorption peaking at 310 nm represented by the wide orange band results from the formation of peroxyxynitrite.

The experimental data are dominated by a strong negative absorption from 194 to 225 nm caused by the removal of ground-state $\text{NO}_3^-(\text{aq})$ molecules by the photolysis pulse. The transient absorption reaches its minimum immediately after termination of the two-photon absorption peak and recovers to 56% of its minimum value on a 2 ps time scale. Concurrent with the removal of ground-state nitrate molecules, strong induced absorption emerges in the spectral range from 230 to 360 nm, as indicated by the red area in Figure 2. This absorption feature appears within 250 fs and rapidly shifts toward shorter wavelengths, approaching the absorption maximum of ground-state $\text{NO}_3^-(\text{aq})$ at 200 nm as the probe delay increases. Similar spectral behavior was observed in the photolysis of $\bullet\text{ClO}_2(\text{aq})$ ⁴² and $\text{CS}_2(\text{aq})$.⁴³ This was assigned to vibrationally relaxing $\bullet\text{ClO}_2$ and CS_2 molecules on the basis of excellent agreement with calculated transient absorption dynamics of these species. Independent resonant Raman spectroscopy studies on photoexcited $\bullet\text{ClO}_2(\text{aq})$ ⁴⁴ further supported this assignment. The lack of potential energy surfaces of $\text{NO}_3^-(\text{aq})$ prevents a comparison with calculated absorption dynamics of vibrationally relaxing $\text{NO}_3^-(\text{aq})$, but on the basis of the strong resemblance with the spectral shifts reported in the well-established cases of $\bullet\text{ClO}_2(\text{aq})$ and $\text{CS}_2(\text{aq})$, we ascribe the induced absorption transient ranging from 230 to 360 nm to vibrationally excited NO_3^- . Consequently, we infer that the excited NO_3^- molecules transfer to the electronic ground state within 250 fs and vibrationally equilibrate during the subsequent 2 ps. The return to the electronic ground state may involve intermediate electronic states, but assuming the Franck–Condon excitation energies of

(37) Thomsen, C. L.; Madsen, D.; Thøgersen, J.; Byberg, J. R.; Keiding, S. R. *J. Chem. Phys.* **1999**, *111*, 703–710.

(38) Thomsen, C. L.; Madsen, D.; Keiding, S. R.; Thøgersen, J. *J. Chem. Phys.* **1998**, *110*, 3453–3462.

(39) Meyerstein, D.; Treinin, A. *Trans. Faraday Soc.* **1961**, *57*, 2104–2112.

(40) Barat, F.; Hickel, B.; Sutton, J. *Chem. Commun.* **1969**, 125–126.

(41) Thomsen, C. L.; Madsen, D.; Keiding, S. R.; Thøgersen, J. *J. Chem. Phys.* **1998**, *110*, 3453–3462.

(42) Thøgersen, J.; Thomsen, C. L.; Poulsen, J. A.; Keiding, S. R. *J. Phys. Chem. A* **1998**, *102*, 4186–4191.

(43) Thomsen, C. L.; Madsen, D.; Thøgersen, J.; Byberg, J. R.; Keiding, S. R. *J. Chem. Phys.* **1999**, *111*, 703–710.

(44) Hayes, S. C.; Philpott, M. P.; Mayer, S. G.; Reid, J. P. *J. Phys. Chem. A* **1999**, *103*, 5534–5546.

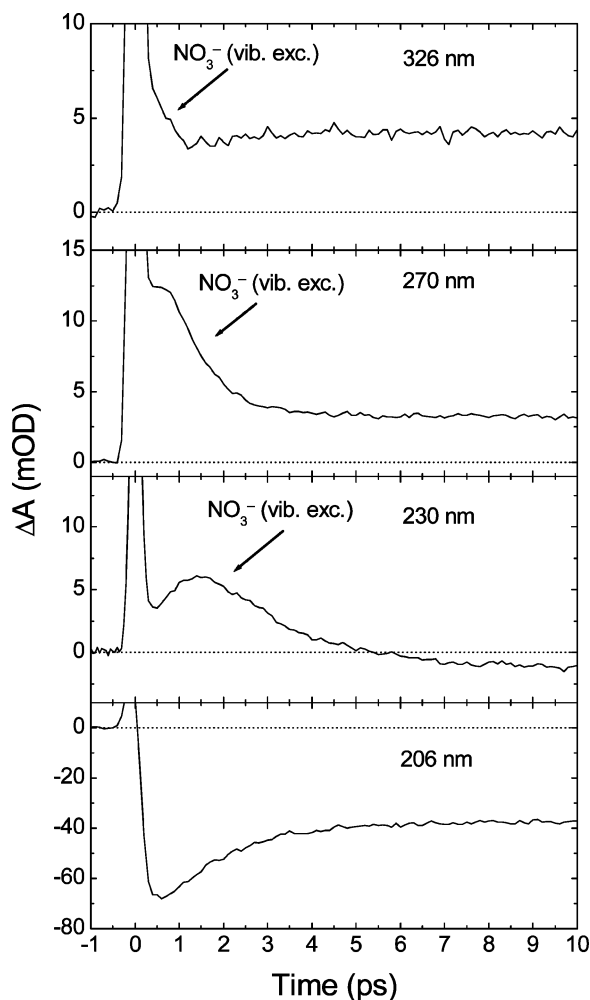


Figure 3. The first 10 ps of the induced transient absorption measured at 326, 270, 230, and 206 nm. The measurement at 326 nm shows the prompt appearance of vibrationally excited NO_3^- , and the formation of peroxyxynitrite lasting 2 ps. At 270 nm, the absorption resulting from vibrationally excited NO_3^- reaches its maximum after 0.6 ps, while the constant absorption after 4 ps originates from peroxyxynitrite. The absorption caused by vibrationally excited NO_3^- appears at longer delays as the wavelength approaches the ground-state NO_3^- absorption maximum at 200 nm, and at 230 nm it peaks after 1.5 ps. This absorption feature is followed by a slightly negative absorption signifying the onset of the nitrate absorption band. The negative absorption at 206 nm indicates the immediate removal and subsequent partial reformation of ground-state NO_3^- occurring on a 2 ps time scale. Note the different absorption scales. See text for details.

the isolated nitrate ion pertain to aqueous solution as well, we assumed that the lowest excited state is about 3.6 eV above the ground state. Hence, the final energy dissipation has to proceed by vibrational relaxation. The incessant spectral shift of vibrationally relaxing NO_3^- and the fact that all measured features will be accounted for by ground-state molecular species exclude significant population of intermediate electronic states having lifetimes in excess of 1 ps. Likewise, the (negative) transient absorption spectrum at 0.5 ps below 230 nm is well approximated by the ground-state NO_3^- (aq) spectrum, indicating that contributions to the transient absorption from excited electronic and vibrational states of nitrate are of little or no importance in this region. Hence, we derive a yield of excited NO_3^- (aq) molecules returning to the electronic ground state of $\Phi(\text{NO}_3^-) = 44 \pm 8\%$ and note that contributions to the absorption from $\bullet\text{O}_2^-$ (aq) or NO^- (aq), to be determined below, reduce this value by less than 2%.

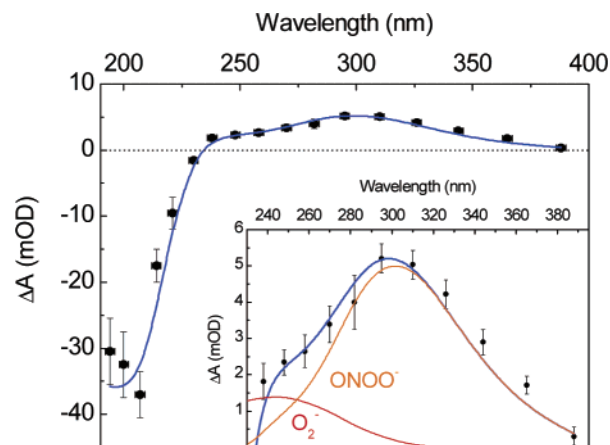


Figure 4. The absorption spectrum measured after 18 ps (squares) fitted by the steady-state absorption spectra of NO_3^- (aq), *cis*- ONOO^- (aq), and $\bullet\text{O}_2^-$ (aq) assuming quantum yields of 44%, 48%, and 8%, respectively.

After 18 ps, the transient spectrum is constant, reflecting that all photoproducts are thermalized. Hence, the remaining 56% of the primary products may be identified by comparing the absorption spectrum after 18 ps shown in Figure 4 with the spectra presented in Figure 1. Apart from the negative induced absorption caused by photoexcitation of NO_3^- , the thermalized absorption spectrum has a pronounced absorption from 250 to 388 nm with a maximum at 295 nm. This absorption profile is nearly identical to the spectrum of *cis*- ONOO^- (aq).^{24,33} The spectrum of *trans*- ONOO^- in Ar-matrices is shifted by about 50 nm relative to its *cis*-conformer. Assuming that a similar spectral shift pertains to aqueous solution, we found that the spectrum of *trans*- ONOO^- (aq) is incompatible with the measured absorption. Because none of the other candidates absorb significantly above 300 nm, the absorption is unambiguously assigned to *cis*- ONOO^- .

The assignment of the ONOO^- (aq) absorption leaves a minor excess absorption from 220 to 270 nm. Detailed analysis reveals that the channels, $\text{NO}_2^- + \text{O}$ (eq 1) and $\bullet\text{NO}_2 + \bullet\text{O}^-$ (eq 2), suggested by previous experiments to be primary reactions, are unable to account for the extra absorption. Guided by photolysis experiments of nitrate salts,⁹ we instead suggest that the superoxide ion, $\bullet\text{O}_2^-$, produced by the reaction



may be responsible for the remaining absorption. We find that a yield of $\Phi(\text{ONOO}^-) = 48 \pm 5\%$ *cis*- ONOO^- (aq) and $\Phi(\bullet\text{O}_2^-) = 8 \pm 3\%$ gives the very satisfactory fit to the thermalized absorption spectrum at 18 ps shown in Figure 4. Hence, no further species are needed to account for the observed absorption. Even though the experimental data are accurately modeled by the $\bullet\text{NO} + \bullet\text{O}_2^-$ channel, the spectral feature tentatively assigned to $\bullet\text{O}_2^-$ (aq) has an uncertainty preventing its unambiguous assignment. Thus, spectral analysis based on the rather poorly determined absorption spectrum of NO^- (aq)³² with yields of $\Phi(\text{NO}^- + \text{O}_2) = 11\%$ and $\Phi(\text{OONO}^-) = 45\%$ also reproduces the experimental data. However, unlike the $\bullet\text{NO} + \bullet\text{O}_2^-$ channel, the formation of $\text{NO}^- + \text{O}_2$ as primary products of the nitrate photolysis has no precedence in the literature. The $\bullet\text{O}_2^-$ (or NO^-) absorption appears after 3 ps, once the obscuring absorption from vibrationally excited NO_3^- has passed, and

remains constant (within the experimental uncertainty) during the subsequent 15 ps. Because of the ambiguity of the dissociation channel, we refer to it as $[\text{NO} + \text{O}_2]^-$ in the remainder of this paper.

The assignment of the absorption spectrum at 18 ps to ONOO^- (aq) and $\bullet\text{O}_2^-$ (or NO^- (aq)) raises the question if species that are not positively identified could be hiding inside the experimental uncertainty. We have addressed this issue by introducing a small variable fraction of the channels $\text{NO}_2^- + \text{O}$ and $\bullet\text{NO}_2 + \bullet\text{O}^-$ into our data analysis. It appears that our data analysis deteriorates if the fraction of the $\text{NO}_2^- + \text{O}$ and $\bullet\text{NO}_2 + \bullet\text{O}^-$ channels exceeds 7% and 5%, respectively. Similarly, if we assume that the unknown extinction coefficient of *trans*- ONOO^- (aq) is similar to that of the *cis*-isomer, we find that a maximum of 5% of the excited NO_3^- molecules are expected to form *trans*- ONOO^- in the primary photolysis.

The *cis*- ONOO^- (aq) absorption transient is seen in Figure 2 as the absorption band centered around 300 nm. The subpicosecond dynamics of ONOO^- is obscured by the overlapping absorption from vibrationally excited nitrate ions. However, absorption pertaining to ONOO^- is clearly present after 1 ps and attains its equilibrium spectrum without the spectral shift characteristic of vibrational relaxation (see Figures 2 and 3 at 326 nm). The fast rise of the ONOO^- concentration indicates that the isomerization occurs within the solvent cage, thus making peroxyxynitrite a primary product of the nitrate photolysis. To further elucidate the dynamics of the ONOO^- concentration, we measured with improved statistical sampling the transient absorption at 310 nm out to 500 ps. The resulting ONOO^- concentration increases steadily by $3 \pm 1\%$ from its value after 1 ps, indicating a slow production of ONOO^- from secondary reactions. The small increase of the ONOO^- concentration in the interval between 1 and 500 ps demonstrates that contributions to the peroxyxynitrite concentration from secondary geminate recombination, like the biologically important radical reaction $\bullet\text{NO} + \bullet\text{O}_2^- \rightarrow \text{ONOO}^-$, are only of minor importance.

Discussion

In accordance with the assignments made in the previous section, we suggest the primary photodynamics of NO_3^- (aq) depicted in Figure 5. When aqueous nitrate is photolyzed at 200 nm (6.2 eV), 44% of the excited NO_3^- molecules return to the vibrationally equilibrated electronic ground state in 2 ps. Concurrently, 48% of the excited NO_3^- molecules isomerize to ONOO^- , while the remaining molecules dissociate to $[\text{NO} + \text{O}_2]^-$.

Two possible reaction pathways may be derived from the transient absorption data with the aid of supplementary results from studies of solid-state and gas-phase nitrate. The measurements show that ONOO^- appears after NO_3^- has reached the vibrationally excited electronic ground state, suggesting that ONOO^- is formed during the vibrational relaxation of ground-state NO_3^- . ONOO^- (aq) has an enthalpy of 1.6 eV relative to ground-state NO_3^- , while the activation energy of the isomerization $\text{ONOO}^- \rightarrow \text{NO}_3^-$ has been estimated to ~ 1.4 eV.^{45–47}

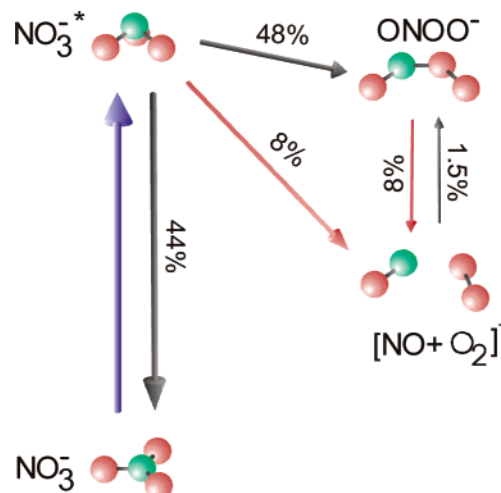


Figure 5. The primary photodynamics of NO_3^- (aq) when excited at 200 nm. The parentheses around $\bullet\text{NO}$ and O_2 indicate that either $\bullet\text{NO}$ or O_2 is negatively charged. The red arrows indicate two alternative reaction paths for the $[\text{NO} + \text{O}_2]^-$ channel. The experiments cannot differentiate between these two reaction paths.

Accordingly, NO_3^- requires in excess of 3 eV to isomerize to ONOO^- . The excited nitrate molecule thus arrives at the isomerization barrier after having dissipated about one-half its 6.2 eV excitation energy to the solvent. At the barrier, the ion may relax into the vibrational manifolds of NO_3^- or ONOO^- . The resulting ONOO^- molecule is formed with 1.4 eV of vibrational energy, which is sufficient for dissociation into $[\text{NO} + \text{O}_2]^-$. Strong coupling between the low-frequency ONOO^- vibrations and the aqueous environment efficiently dissipates this excess energy to the solvent, resulting in the rapidly thermalized ONOO^- transient absorption spectrum observed experimentally.^{48–50}

Alternatively, early isomerization via states connecting the excited NO_3^- ion with the electronic ground state of ONOO^- precedes the vibrational energy dissipation. According to this picture, the excitation energy of the newly formed ONOO^- isomer is well above its dissociation energy, and dissociation into $[\text{NO} + \text{O}_2]^-$ is possible. However, in most cases, the water cage inhibits the free dissociation, thereby forcing the majority of the excited molecules to remain inside the cage as NO_3^- or ONOO^- . Only for cage configurations where the solvent barrier is sufficiently low may the dissociation be completed and the fragments escape. For this explanation to comply with the absence of absorption from vibrationally excited ONOO^- , the vibrational deexcitation is required to finish within 1 ps. Although this is remarkably fast, the short vibrational relaxation time of NO_3^- (aq) combined with the stronger solvent–solute coupling of the low-frequency modes of ONOO^- ^{48–50} suggest that sub-picosecond relaxation of ONOO^- (aq) could be feasible.

In addition to direct photoisomerization within the solvent cage, a small contribution to the ONOO^- concentration from diffusive recombination is observed. The secondary formation

(45) Manuszak, M.; Koppenol, W. H. *Thermochim. Acta* **1996**, *273*, 11–15.

(46) Ray, J. D. *J. Inorg. Nucl. Chem.* **1962**, *24*, 1159–1162.

(47) Knak Jensen, S. J.; Mátyus, P.; McAllister, M. A.; Csizmadia, I. G. *J. Phys. Chem. A* **2001**, *105*, 9029–9033.

(48) The lowest vibration frequency of ONOO^- is $\sim 50\%$ smaller than that of NO_3^- . Tsai, J.-H. M.; Harrison, J. G.; Martin, J. C.; Hamilton, T. P.; der Woerd, M. V.; Jablonsky, M. J.; Beckman, J. S. *J. Am. Chem. Soc.* **1994**, *116*, 4115–4116.

(49) Larsen, J.; Madsen, D.; Thøgersen, J.; Poulsen, T. D.; Keiding, S. R. *J. Chem. Phys.* **2002**, *116*, 7997–8005.

(50) Harris, A. L.; Brown, J. K.; Brown, C. B. *Annu. Rev. Phys. Chem.* **1988**, *39*, 341–366.

of ONOO⁻ may result from the diffusion-limited radical reaction⁵¹



or from the reaction



If indeed the reactants in eq 6 are produced in the primary photolysis, they may be formed in the triplet ground state, ³NO⁻, ³O₂, or singlet excited state, ¹NO⁻, ¹O₂. The spin-allowed recombination of ground-state ³NO⁻ with ³O₂ is known to result in a near-diffusion limited ($k = 2.7 \times 10^9 \text{ M}^{-1} \text{ s}^{-1}$) production of ground-state peroxyxynitrite, ¹ONOO⁻.⁵² On the other hand, the rate of the reaction ¹NO⁻ + ¹O₂ → ONOO⁻ is, to the best of our knowledge, unknown. ¹NO⁻ is a very strong base ($\text{p}K_{\text{a}} \approx 23$),⁵² and protonation by the surrounding water molecules would consequently lead to the rapid formation of hydroxyl anions according to the reaction⁵²



OH⁻(aq) has a relatively intense absorption band below 210 nm⁵³ and is in principle detectable by our far-UV femtosecond spectrometer, but the small yield of NO⁻ together with the large absorption background from nitrate prevents its identification. Accordingly, the present measurements are unable to determine the spin multiplicity of NO⁻. Assuming reactions 5 and 6 are diffusion controlled, we have simulated the recombination processes using a spherical symmetric diffusion process⁵⁴ and adopted reasonable parameters for the diffusion constants ($D = 2 \times 10^{-5} \text{ cm}^2/\text{s}$), reaction radius (5 Å), and initial separation of the fragments (10 Å).^{55,56} We find that both reactions 5 and 6 can account quantitatively for the increase in ONOO⁻ concentration. The associated decrease in the concentration of [•]O₂⁻ or NO⁻ is about 15% in 500 ps. Although such a decrease is easily accommodated by the experimental data, the relatively large uncertainty prevents its definite confirmation.

In contrast to earlier studies,^{4,7,8,16,17,57} the present measurements do not find NO₂⁻ or [•]O⁻ among the primary photoproducts.

Although not observed experimentally, it is possible that [•]NO₂ + [•]O⁻ and NO₂⁻ + O briefly exist as transient dissociation fragments inside the solvent cage. If so, the experimental data clearly show that they disappear within 250 fs, likely through recombination. Hence, the reactions NO₃⁻ + $h\nu \rightarrow$ NO₂⁻ + O (eq 1) and $h\nu +$ NO₃⁻ → [•]NO₂ + [•]O⁻ (eq 2) have only little, if any, significance for the primary photo-dynamics in aqueous solution.

Instead, we detect the formation of [•]O₂⁻ (or NO⁻) and measure a primary quantum yield of ONOO⁻, which is 5 times that reported by Mark et al.⁴ The different ONOO⁻ quantum yields may in part be related to the different excitation wavelengths used in the two studies. The present investigation excites the $\pi \rightarrow \pi^*$ transition at 200 nm, while in the work by Mark et al.⁴ nitrate was photolyzed right at the overlap between the $\pi \rightarrow \pi^*$ and $n \rightarrow \pi^*$ transitions at 254 nm. The ONOO⁻ quantum yield resulting from the $n \rightarrow \pi^*$ excitation is expected to be significantly lower than that following the excitation of the $\pi \rightarrow \pi^*$ transition¹⁰ and is thus in qualitative agreement with the lower yield observed by Mark et al.⁴ Moreover, the femtosecond time resolution of the present work eliminates competing reactions with products from other reactions and impurity species such as for instance O₂. The smaller ONOO⁻ quantum yield observed by steady-state photolysis⁴ may therefore reflect peroxyxynitrite depleting secondary reactions.

Conclusions

The femtosecond transient absorption measurements presented here lead to a much simplified reaction scheme for the primary UV photolysis of aqueous NO₃⁻. Upon excitation of NO₃⁻(aq), 44 ± 8% of the molecules return nonadiabatically to the electronic ground state within 250 fs. The remaining 56% of the excited molecules proceed to form *cis*-ONOO⁻ (48%) or dissociate to [•]NO + [•]O₂⁻ (8%) or NO⁻ + O₂ (11%). The peroxyxynitrite isomer attains its ground state in 1 ps as a primary photoproduct of the NO₃⁻ photolysis, and the relative contribution to the peroxyxynitrite yield from secondary reactions during the subsequent 500 ps amounts to only 3%. Contrary to previous studies, the present investigations find no evidence of NO₂⁻ + O or [•]NO₂ + [•]O⁻, indicating that the NO₂⁻ formation observed in steady-state photolysis experiments must be due to subsequent reactions.^{58,59}

Acknowledgment. The outstanding technical support of Per Strand is highly appreciated.

JA030135F

- (51) Kobayashi, K.; Miki, M.; Tagawa, S. *J. Chem. Soc., Dalton Trans.* **1995**, 2885–2889.
 (52) Shafirovich, V.; Lyman, S. V. *Proc. Natl. Acad. Sci. U.S.A.* **2002**, *99*, 7340–7345.
 (53) Nielsen, S. O.; Michael, B. D.; Hart, E. J. *J. Phys. Chem.* **1976**, *80*, 2482–2488.
 (54) Krissinel, E. B.; Agmon, N. *J. Comput. Chem.* **1996**, *17*, 1085–1098.
 (55) Madsen, D.; Thomsen, C. L.; Poulsen, J. A.; Poulsen, Knak Jensen, S. J.; Thøgersen, J.; Keiding, S. R.; Krissinel, E. B. *J. Phys. Chem.* **2003**, *107*, in press.
 (56) *CRC Handbook of Chemistry and Physics*, 74th ed.; CRC Press: Boca Raton, FL, 1993; pp 5–91.

- (57) Edwards, J. O.; Plumb, R. C. In *Progress in Inorganic Chemistry*; Karlin, K. D., Ed.; John Wiley & Sons: New York, 1994; Vol. 41, pp 599–635.
 (58) Merényi, G.; Lind, J.; Goldstein, S.; Czapski, G. *J. Phys. Chem. A* **1999**, *103*, 5685–5691.
 (59) Kissner, R.; Koppenol, W. H. *J. Am. Chem. Soc.* **2002**, *124*, 234–239.